Diruthenium compounds of thiol capped oligo(phenyleneethynyl) ligand: Synthesis and characterization

Jie-Wen Ying, Tong Ren *

Department of Chemistry, Purdue University, 560 Oval Drive, West Lafayette, IN 47907, USA

Abstract

Reactions between $Ru_2(DMBA)_4(NO_3)_2$ and OPEn-S-TMSE ligand under weak base conditions afford *trans*-$Ru_2(DMBA)_4$(OPEn-S-TMSE)$_2$ compounds, where DMBA is N,N'-dimethylbenzamidinate, TMSE is trimethylsilylethylene, and OPEn are $-C\equiv CC_6H_4-$ (**1**), $-C\equiv C(2,5-(CH_3O)_2C_6H_2)-(C\equiv CC_6H_4)-$ (**2**) and $-(C\equiv CC_6H_4)-C\equiv C(2,5-(CH_3O)_2C_6H_2)-(C\equiv CC_6H_4)-$ (**3**). Molecular structures of compounds **1** and **2** were determined by X-ray diffraction, which revealed the extended rigid rod topology and coplanarity of phenylene-ethynye units in **1** and **2**. Electrochemical and optical energy gaps of compounds **1**–**3** were estimated to be 1.57 eV and *ca.* 1.43 eV, respectively, from voltammetric and absorption spectral measurements.
© 2006 Elsevier B.V. All rights reserved.

Keywords: Diruthenium; OPEs; Molecular wires

1. Introduction

Conjugated oligomers have drawn intense interest from chemists and material scientists as the lead candidates to replace silicon semiconductor in many (opto)electronic applications [1], including photovoltaics [2], organic field effect transistors [3], electrochemical and fluorescent sensors [4], and molecular wires and devices [5]. Among many established families of organic oligomers, both linear and branched OPEs (OPE = oligo(phenyleneethynylene)) have been heavily investigated due to their structural rigidity and extensive π-conjugation [6], and the latter feature renders OPEs as efficient scaffolds for energy transfer over long distances [7]. It has been noted that figures of merit of materials may be improved over pure organic oligomers when metal centers are incorporated into conjugated oligomers either in the main chain or as the side chain pendants [8]. Transition metal compounds with ligand containing OPEn fragment (OPE$n = (C\equiv CC_6H_4)_n$, $n \geqslant 2$) have become increasingly common in recent years, and examples

include the α,ω-ferrocenyl-OPEn-thioether series [9], an Os$_3$ cluster with a σ-S–$S(C_6H_4C\equiv C)_2$Ph ligand [10], and various Ru(II) and Au(I) complexes coordinated by OPEn ligands in both σ- and η^2 modes [11]. Our laboratory is interested in developing molecular wires based on linear metal-alkynyl species with a focus on diruthenium compounds supported by N,N'-bidentate ligands [12,13]. These diruthenium alkynyl species exhibit small electrochemical and optical energy gaps [14,15] and mediate efficient charge transfer [16–18]. Corroborating results reported for other metal-containing OPE molecules [19], recent STM study of $Ru_2(ap)_4(C\equiv CC_6H_4)_2S$ (ap is 2-anilinopyridinate) embedded in the SAM of C11 alkane thiol revealed a markedly improved molecular conductance over OPE molecule of comparable length [12,20]. Also worthy of mentioning is the recent demonstration of enhanced charge transfer in trinuclear and pentanuclear metal complexes and single molecule transistors based on this type compounds [21]. The promising result based on $Ru_2(ap)_4(C\equiv CC_6H_4)_2S$ inspires further study of Ru$_2$ bis-alkynyl wires, for which diruthenium compounds supported by symmetric DMBA (N,N'-dimethylbenzamidinate) ligand is superior to $Ru_2(ap)_4$ from both synthetic and structural perspectives.

* Corresponding author. Tel.: +1 765 494 5466; fax: +1 765 494 0239.
  E-mail address: tren@purdue.edu (T. Ren).
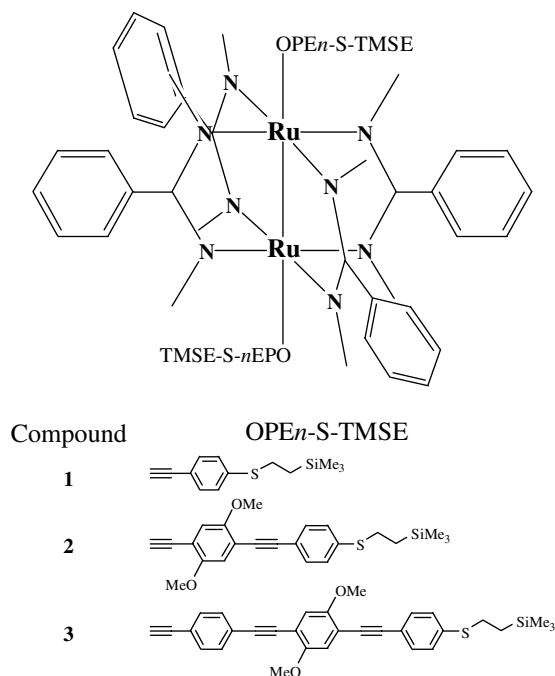
Scheme 1. Wire-like $Ru_2(DMBA)_4(OPEn)_2$ compounds.

We previously communicated the assembly of Au nanoparticles with a series of $Ru_2(DMBA)_4(OPEn\text{-}S\text{-}TMSE)_2$ complexes [22], where OPEn is oligo(phenyleneethynylene) with n indicating the degree of oligomerization and TMSE is trimethylsilylethylene (Scheme 1). Reported herein are detailed description of the synthesis, structural study and voltammetric properties of these novel diruthenium compounds.

2. Results and discussion

2.1. Synthesis

Thiol capped OPE1-S-TMSE and OPE2-S-TMSE ligands were prepared following the literature procedures

[23,24], and OPE3-S-TMSE ligand was prepared from a Sonogashira coupling reaction between trimethylsilyl 4-ethynyliodobenzene and OPE2-S-TMSE. Trimethylsilylethylene (TMSE) was chosen as the thiol protection group because of its superior chemical stability over acetyl protection group, and methoxy phenyl substituents were introduced in both OPE2 and OPE3 ligands to improve the solubility of the resultant $Ru_2(DMBA)_4$ compounds. Compounds 1–3 were prepared from reactions between $[Ru_2(DMBA)_4](NO_3)_2$ and the appropriate OPEn-S-TMSE ligand in the presence of Et_3N, and purified on silica column. Compounds 1–3 are red, diamagnetic crystalline materials, and soluble in common organic solvents.

2.2. Molecular structures

Molecular structures of compounds 1 and 2 determined via single crystal X-ray diffraction are shown in Figs. 1 and 2, respectively, and some selected bond lengths and angles are collected in Table 1. In both cases, the asymmetric unit contains one half of the diruthenium molecule, and a crystallographic inversion center bisecting the Ru–Ru bond relates one half of the molecule to the other half. It is clear from Figs. 1 and 2 that the coordination sphere of Ru_2 center retains the paddlewheel motif of $Ru_2(DMBA)_4(NO_3)_2$ precursor. The Ru–Ru bond lengths determined, 2.4597(8) (1) and 2.4626(8) Å (2), are comparable with those found for the related $Ru_2(DMBA)_4(C\equiv CAr)_2$ type compounds [25,26], and consistent with the presence of a Ru–Ru single bond [27]. Close examination of Table 2 revealed that the first coordination sphere of Ru_2 core exhibits significant distortion from the D_{4h} symmetry expected for an idealized paddlewheel motif: markedly nonlinear $Ru'–Ru–C_\alpha$ angles and large variances in both Ru–N bond lengths and $Ru'–Ru–N$ angles. This type distortion is common among Ru2(III)-bisalkynyl species [12,13,28], and has an origin of second-order Jahn–Teller effect [29].
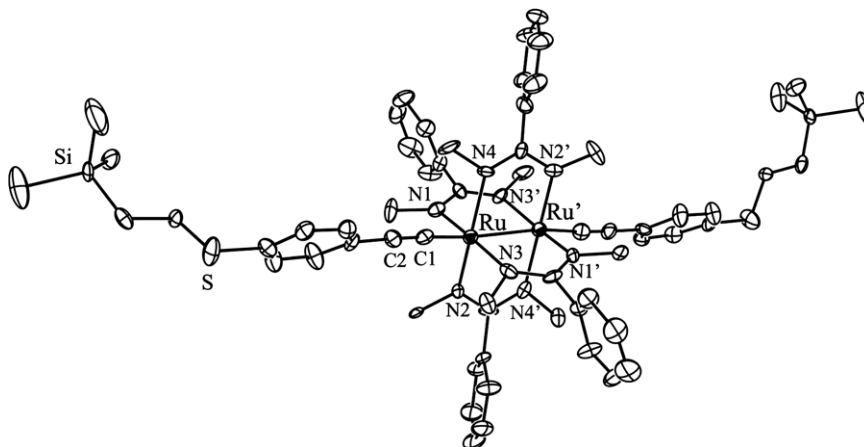
Fig. 1. ORTEP plot of compound 1 at 30% probability level. Hydrogen atoms were omitted for clarity.
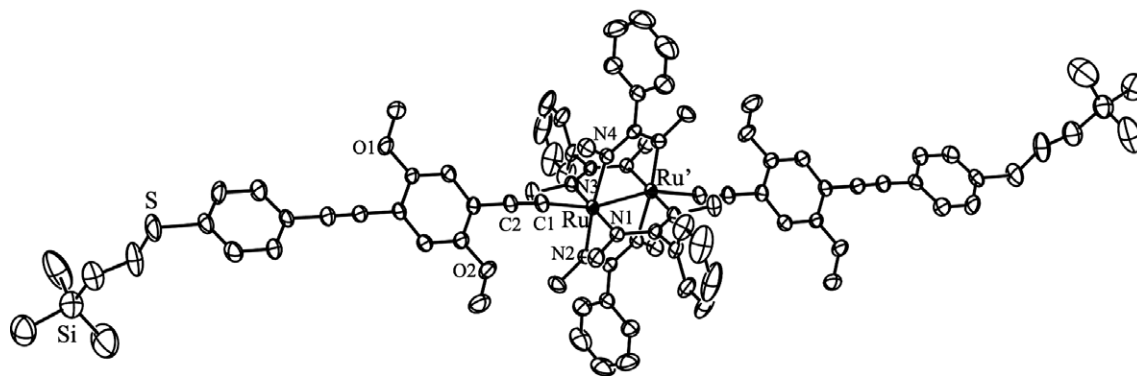
Fig. 2. ORTEP plot of compound **2** at 30% probability level. Hydrogen atoms were omitted for clarity.

Table 1
Selected bond lengths (Å) and angles (°) for compounds **1** and **2**

	1	**2**
Ru–Ru′	2.4597(8)	2.4626(8)
Ru–C1	1.995(5)	1.968(5)
Ru–N1	1.907(14)	1.996(4)
Ru–N2	2.074(13)	1.977(4)
Ru–N3	2.181(12)	2.103(4)
Ru–N4	2.064(14)	2.101(4)
C1–C2	1.204(7)	1.207(7)
C1–Ru–Ru′	160.19(17)	161.38(17)
C2–C1–Ru	172.6(5)	174.6(5)
N1–Ru–Ru′	96.5(4)	95.73(11)
N2–Ru–Ru′	96.3(4)	97.08(12)
N3–Ru–Ru′	80.0(4)	80.09(11)
N4–Ru–Ru′	79.4(4)	78.86(11)

In the structure of **1**, two phenyleneethyne units are related by an inversion center and hence rigorously coplanar. While similar coplanarities between phenyleneethyne units related by inversion are expected in molecule **2**, it is interesting to note that two phenyleneethyne units within the same OPE2 are nearly coplanar as well. There are

Table 2
Crystallographic parameters for compounds **1** · C_6H_{14} and **2** · C_6H_{14}

	1 · C_6H_{14}	**2** · C_6H_{14}
Formula	$C_{68}H_{92}N_8Ru_2S_2Si_2$	$C_{88}H_{108}N_8O_4Ru_2S_2Si_2$
Fw	1343.9	1664.3
Space group	C2	P$\bar{1}$
a (Å)	11.219(2)	12.976(1)
b (Å)	18.897(3)	13.840(1)
c (Å)	16.872(3)	14.245(1)
α (°)		106.950(2)
β (°)	106.173(3)	104.661(2)
γ (°)		107.477(2)
Volume (Å³)	3435.6(9)	2165.2(3)
Z	2	1
D_{calc} (g cm⁻³)	1.299	1.276
μ (mm⁻¹)	0.580	0.477
Radiation	Mo Kα	Mo Kα
T (K)	300(2)	300(2)
R_1, wR_2 ($I > 2\sigma(I)$)	0.041, 0.095	0.060, 0.12

about 10 structurally characterized metal-OPE*n* ($n \geqslant 2$) compounds that are mostly mono-OPE species and metal centers include Ru(II), Ni(II), Pd(II), Pt(II), Ag(I) and Au(I) [30]. Examination of the deposited data in CSD revealed that the twist between phenyleneethyne units is prevalent. In the only related bis-OPE*n* example, *trans*-Pt(PBu$_3$)$_2$(OPE2)$_2$ [31], all phenyleneethyne units are close to be coplanar. The *near* coplanarity observed in *trans*-Pt(PBu$_3$)$_2$(OPE2)$_2$, compounds **1** and **2** may indicate an extended conjugation over the entire OPE*n*-M-OPE*n* fragment, although the packing effect may also contribute to the observed coplanarity. Last but not the least, the S···S distances in compounds **1–3** are critical for the assessment of their molecular wire characteristics, and values determined from structure refinements are 20.8 and 34.4 Å for **1** and **2**, respectively, and the estimated value for **3** is about 48 Å.

2.3. Electrochemical and spectroscopic properties

The ability of conjugated species to function as molecular wires is intimately related to their redox characteristics, and those of compounds **1–3** were examined via cyclic voltammetric technique. As shown in Fig. 3, compounds **1–3** display nearly identical cyclic voltammograms that consist of a reversible oxidation (**A**) and a (quasi)reversible reduction (**B**). As the OPE*n* ligand elongates, the reduction couple (**B**) becomes less reversible, and an additional anodic wave at more positive potential (**C**) is noticeable in the CV of **3**, indicating partial dissociation of OPE3 ligand on reduction [15]. On the other hand, features of the oxidation couple (**A**) remain invariant across the series. Based on the electrode potentials, the HOMO–LUMO gaps of the solvated Ru$_2$-OPE*n* were estimated to be *ca.* 1.57 V from the relationship of $E_g = E_{1/2}(A) - E_{1/2}(B)$ [32].

As shown in Fig. 4, compound **1** exhibits an intense band at 506 nm and an NIR band at 893 nm with moderate intensity, and the combination of both results in the dark red appearance of the compound. The previously studied Ru$_2$(DMBA)$_4$(C≡CAr)$_2$ type compounds display similar Vis–NIR spectra of absorptions at 500–510 nm and 850–
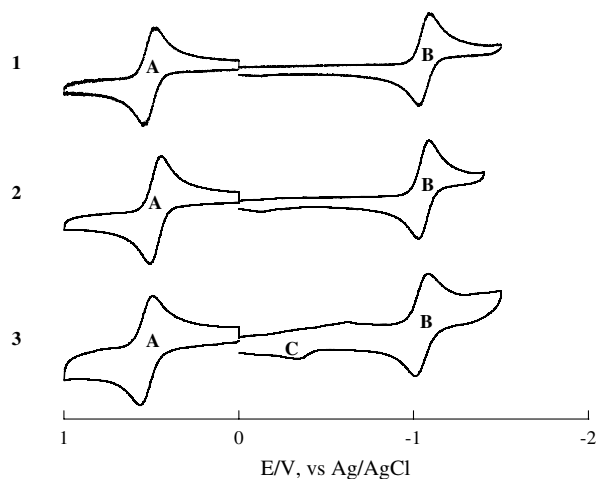
Fig. 3. Cyclic voltammograms of compounds 1–3 recorded in THF at a scan rate of 0.10 V/s.
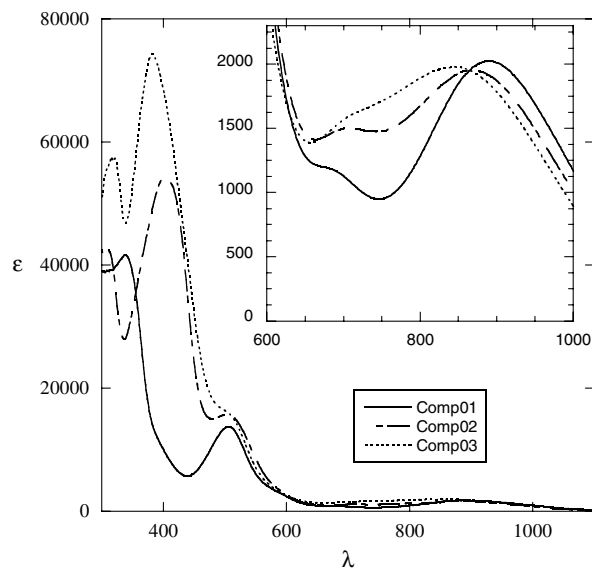

Fig. 4. Vis–NIR spectra of compounds 1–3 recorded in THF solution.

870 nm [25]. According to the TD-DFT (B3LYP) analysis of $Ru_2(DMBA)_4(C\equiv CFc)_2$ [18], the lowest energy absorption is attributed to the $\pi^*(Ru_2) \rightarrow \delta^*(Ru_2)$ transition, where the axial alkynyl ligand contributes through the antibonding overlap between $\pi(C\equiv C)$ and $\pi^*(Ru_2)$. The absorption around 510 nm is likely a mixture of both the $L(N) \rightarrow \delta^*(Ru_2)$ and $\delta(Ru_2) \rightarrow \delta^*(Ru_2)$ transitions. The free ligand TMS-OPE1-S-TMSE displays a $\pi \rightarrow \pi^*$ transition at 294 nm (4.22 eV) (see Section 4). The corresponding transition in compound 1 occurs around 338 nm (3.67 eV), implying a 0.55 eV red-shift upon metallation. Compounds 2 and 3 exhibit very intense $\pi \rightarrow \pi^*$ bands at 403 nm (3.08 eV) and 382 nm (3.25 eV), respectively, while the free ligands TMS-OPE2-S-TMSE and TMS-OPE3-S-TMSE display lowest $\pi \rightarrow \pi^*$ bands at 373 nm (3.32 eV) and 377 nm (3.29 eV), respectively. These data seem to indicate

that the red-shift of $\pi \rightarrow \pi^*$ band due to metallation gradually diminishes upon the extension of OPEn ligand. As shown by the inset in Fig. 4, the lowest energy band at 893 nm (1.39 eV) in 1 has been blue-shifted to 867 nm (1.43 eV) in 2 and 846 nm (1.47 eV) in 3, while the intensity remains the same.

3. Conclusion

A series of soluble and thiol-capped diruthenium-OPEn compounds was prepared and characterized with X-ray and voltammetric techniques. These novel compounds bear strong similarity in both the structural and voltammetric characteristics to the series of $Ru_2(DMBA)_4(C_{2n}Fc)_2$ compounds, where highly efficient hole transfer was demonstrated through bulk solution spectroelectrochemistry studies [17,18]. Hence, compounds 1–3 may exhibit enhanced molecular conductance over pure OPEs of comparable lengths, and the measurements of single molecule conductance are being pursued with a variety of nano-junction techniques.

4. Experimental

$Pd(PPh_3)_2Cl_2$ was purchased from Aldrich, 1-bromothiophenol, diisopropylamine, triethylamine, iodine, 1,4-dimethoxybenzene, vinyltrimethylsilane, tert-butyl peroxide and copper iodide from ACROS, trimethylsilylacetylene and trimethylsilyl ethynyliodobenzene from GFS, and silica gel from Merck. $Ru_2(DMBA)_4(NO_3)_2$ [33] and OPE1-S-TMSE [23] were prepared according to the literature. THF was distilled over Na/benzophenone under an N_2 atmosphere prior to use. ^1H NMR spectra were recorded on a Bruker AVANCE300 NMR spectrometer, with chemical shifts (δ) referenced to the residual $CHCl_3$. Infrared spectra were recorded on a Perkin–Elmer 2000 FT-IR spectrometer using KBr disks. UV–Vis–NIR spectra were obtained with either a Perkin–Elmer Lambda-900 UV–Vis–NIR spectrophotometer or a Cary300 UV–Vis spectrometer. Cyclic voltammograms were recorded in 0.2 M $(n\text{-}Bu)_4NPF_6$ solution (THF, N_2-degassed) on a CHI620A voltammetric analyzer with a glassy carbon working electrode (diameter = 2 mm), a Pt-wire auxiliary electrode and a Ag/AgCl reference electrode. Typical CV was recorded from 0 V to more negative potential during the cathodic scan, and from 0 V to more positive potential during the anodic scan. The concentration of diruthenium species is always 1.0 mM. The ferrocenium/ferrocene couple was observed at 0.586 V (vs. Ag/AgCl) under experimental conditions.

4.1. Synthesis of TMSOPE2-S-TMSE

A solution of 0.500 g (1.4 mmol) of 2-iodo-5-(trimethylsilyl)ethynyl-1,4-dimethoxybenzene, which was prepared using the literature procedure with slight modification [23], and 0.325 g (1.39 mmol) of OPE1-S-TMSE, 0.139 g

(0.2 mmol) of $Pd(PPh_3)_2Cl_2$, 0.139 g (0.70 mmol) of CuI, 30 mL of diisopropylamine and 30 mL of THF was stirred under argon at 70 °C overnight. The solvents were removed and the residue was purified by column chromatography with CH_2Cl_2/hexanes (1/5, v/v) to yield 0.57 g (88%) of pure product. Data for TMS-OPE2-S-TMSE: ^{1}H NMR: 7.47 (d, 2H, aromatic), 7.25 (m, 2H, aromatic), 6.98 (d, 2H, aromatic), 3.88 (d, 6H, $CH_3O–$), 3.02–2.98 (m, 2H, $TMSCH_2CH_2S–$), 0.98–0.95 (m, 2H, $TMSCH_2CH_2S–$), 0.29 (s, 9H, $–Si(CH_3)_3$), 0.09 (s, 9H, $–Si(CH_3)_3$). UV–Vis (THF), λ_{max} (nm, ε (M^{-1} cm^{-1})): 323(14 900), 362(19 200), 373(17 100). UV–Vis (THF) of TMS-OPE1-S-TMSE, λ_{max}(nm, ε (M^{-1} cm^{-1})): 294(27 300).

4.2. Synthesis of TMS-OPE3-S-TMSE

A mixture of 0.500 g (1.27 mmol) of OPE2-S-TMSE (prepared from desilylation of TMS-OPE2-S-TMSE with excess of K_2CO_3 in THF/CH_3OH (1/1, v/v)), and 0.38 g (1.27 mmol) of trimethylsilyl ethynyliodobenzene, 0.150 g (0.21 mmol) of $Pd(PPh_3)_2Cl_2$, 0.150 g (0.8 mmol) of CuI, 40 mL of diisopropylamine and 40 mL of THF was stirred under argon at 70 °C overnight. Solvents were removed and the residue was purified by column chromatography with CH_2Cl_2/hexanes (1/5, v/v) to yield 0.550 g (76%) of pure product. Data for TMS-OPE3-S-TMSE ^{1}H NMR: 7.50–7.42 (m, 7H, aromatic), 7.25–7.22 (m, 1H, aromatic), 7.01 (d, 2H, aromatic), 3.89 (d, 6H, $CH_3O–$), 3.01–2.95 (m, 2H, $TMSCH_2CH_2S–$), 0.97–0.91 (m, 2H, $TMSCH_2CH_2S–$), 0.25 (s, 9H, $–Si(CH_3)_3$), 0.05 (s, 9H, $–Si(CH_3)_3$). UV–Vis (THF), λ_{max}(nm, ε (M^{-1} cm^{-1})): 322(42 900) and 377(52 900).

4.3. Synthesis of compound 1

To a suspension of 0.200 g (0.22 mmol) of $Ru_2(DMBA)_4(NO_3)_2$ in 50 mL THF was added 0.500 g (2.14 mmol) of OPE1-S-TMSE and 20 mL of Et_3N. The reaction mixture was stirred at room temperature for 2 h. Upon the solvent removal, the residue was triturated with methanol and filtered to afford a red powder 0.180 g (73%). Data for $Ru_2(DMBA)_4(OPE1-S-TMSE)_2$: ^{1}H NMR: 7.42–7.36 (m, 12H, aromatic), 7.14 (d, 4H, aromatic), 6.99 (t, 12H, aromatic), 3.26 (s, 24H, MeN–), 2.85–2.79 (m, 4H, $TMSCH_2CH_2S–$), 0.87–0.80 (m, 4H, $TMSCH_2CH_2S–$), 0.03 (s, 18H, $–Si(CH_3)$); MS-FAB (m/e, based on ^{101}Ru): 1262 [M^+]; Vis–NIR, λ_{max}(nm, $\varepsilon(M^{-1}$ cm^{-1})): 893(1780), 506(13 750), 338(41 670); IR (cm^{-1}), $\upsilon(C≡C)$ 2078(s); electrochemistry, $E_{1/2}/V$, $\Delta E_p/V$, $i_{backward}/i_{forward}$: **A**, 0.517, 0.057, 0.96; **B**, −1.060, 0.057, 0.94.

4.4. Synthesis of compound 2

To a suspension of 0.160 g (0.18 mmol) of $Ru_2(DMBA)_4(NO_3)_2$ in 50 mL THF was added 0.496 g (1.06 mmol) of OPE2-S-TMSE and 20 mL Et_3N. The reaction mixture was stirred at room temperature for 2 h. Upon the solvent removal, the residue was purified by column chromatography, and eluted with THF/hexanes (1/5, v/v) to afford 0.108 g (38%) title compound as red crystalline solid. Data for $Ru_2(DMBA)_4(OPE2-S-TMSE)_2$: ^{1}H NMR: 7.48–7.41 (m, 16H, aromatic), 7.21 (d, 4H, aromatic), 7.05 (d, 8H, 6.90 aromatic), 6.89 (s, 2H, aromatic), 6.63 (s, 2H, aromatic), 3.80 (s, 6H, $CH_3O–$), 3.70 (s, 6H, $CH_3O–$), 3.35 (s, 24H, MeN–), 2.99–2.94 (m, 4H, $TMSCH_2CH_2S–$), 0.95–0.83 (m, 4H, $TMSCH_2CH_2S–$), 0.04 (s, 9H, $–Si(CH_3)_3$), 0.01 (s, 9H, $–Si(CH_3)_3$); MS-FAB (m/e, based on ^{101}Ru): 1581 [M^+]; Vis–NIR, λ_{max}(nm, ε (M^{-1} cm^{-1})): 867(1740), 502 (15 730), 403(54 300); IR (cm^{-1}), $\upsilon(C≡C)$: 2069(s); electrochemistry, $E_{1/2}/V$, $\Delta E_p/V$, $i_{backward}/i_{forward}$: **A**, 0.478, 0.061, 0.99; **B**, −1.056, 0.061, 0.89.

4.5. Synthesis of compound 3

To a suspension of 0.200 g (0.22 mmol) of $Ru_2(DMBA)_4(NO_3)_2$ in 50 mL THF was added 0.680 g (1.38 mmol) of OPE3-S-TMSE, prepared from desilylation of TMS-OPE3-S-TMSE with excess of K_2CO_3 in THF/CH_3OH (1/1, v/v), and 20 mL Et_3N. The reaction mixture was stirred at room temperature for 2 h. Upon the solvent removal, the residue was purified by column chromatography, and eluted with THF/hexanes (1/5, v/v) to afford 0.130 g title compound (33%). Data for $Ru_2(DMBA)_4(OPE3)_2$: ^{1}H NMR: 7.49–7.39 (m, 20H, aromatic), 7.28–7.26 (m, 4H, aromatic), 6.93–7.05 (m, 16H, 6.90 aromatic), 3.90 (s, 12H, $CH_3O–$), 3.32 (s, 24H, MeN–), 3.03–2.97 (m, 4H, $TMSCH_2CH_2S–$), 0.99–0.86 (m, 4H, $TMSCH_2CH_2S–$), 0.07 (s, 9H, $–Si(CH_3)_3$), 0.02 (s, 9H, $–Si(CH_3)_3$); MS-FAB (m/e, based on ^{101}Ru): 1283 [$M^+ –$ OPE3]; Vis–NIR, λ_{max}(nm, ε (M^{-1} cm^{-1})): 846 (2024), 505(sh), 381(74 320); IR (cm^{-1}), $\upsilon(C≡C)$: 2069 (s); electrochemistry, $E_{1/2}/V$, $\Delta E_p/V$, $i_{backward}/i_{forward}$: **A**, 0.530, 0.073, 0.99; **B**, −1.047, 0.075, 0.89.

4.6. Structure determination

Single crystals were obtained by slow diffusion of hexanes into THF solution (**1**) or benzene solution (**2**). X-ray intensity data were measured at 300 K on a Bruker SMART 1000 CCD-based X-ray diffractometer system using Mo Kα ($\lambda = 0.71073$ Å). For data collection, a red plate of **1** with approximate dimensions $0.28 \times 0.13 \times 0.04$ mm^3 was sealed in a 0.2 mm capillary with mother liquor, while a red plate of **2** with approximate dimensions $0.19 \times 0.13 \times 0.03$ mm^3 cemented to a quartz fiber with epoxy glue. Data were measured using omega scans of 0.3° per frame for 30 s for **1** and 40 s for **2** so that a hemisphere (1271 frames) was collected. The frames were integrated with the Bruker SAINT$^©$ software package [34] using a narrow-frame integration algorithm, which also corrects for the Lorentz and polarization effects. Absorption corrections were applied using SADABS.

Structures were solved and refined using the Bruker SHELXTL$^{©}$ (Version 5.1) software package [35] in space groups of *C*2 (**1**) and *P*1̄ (**2**). Positions of all non-hydrogen atoms were revealed by direct method. All non-hydrogen atoms are anisotropic and the hydrogen atoms were put in calculated positions and riding mode. Each structure was refined to convergence by least squares method on F^2, SHELXL-93, incorporated in SHELXTL.PC V 5.03. Crystallographic data are given in Table 2.

Appendix A. Supporting information

Crystallographic data for the structural analysis have been deposited with the Cambridge Crystallographic Data Center, CCDC 246907 and 246908 for compounds **1** and **2**, respectively. Copies of this information may be obtained free of charge from The Director, CCDC, 12 Union Road, Cambridge CB2 1EZ, UK, fax: +44-1233-336033; email: deposit@ccdc.cam.ac.uk or www:http://ccdc.cam.ac.uk. Supplementary data associated with this article can be found, in the online version, at doi:10.1016/j.jorganchem.2006.06.005.

References

[1] K. Mullen, G. Wegner, Electronic Materials: the Oligomer Approach, Wiley VCH, Weinheim; New York, 1998.

[2] J.L. Segura, N. Martín, D.M. Guldi, Chem. Soc. Rev. 34 (2005) 31.

[3] A. Facchetti, M.H. Yoon, T.J. Marks, Adv. Mater. 17 (2005) 1705.

[4] D.T. McQuade, A.E. Pullen, T.M. Swager, Chem. Rev. 100 (2000) 2537;
T.M. Swager, Acc. Chem. Res. 31 (1998) 201.

[5] M.A. Reed, T. Lee (Eds.), Molecular Nanoelectronics, American Scientific Publishers, Stevenson Ranch, CA, 2003;
J.M. Tour, Acc. Chem. Res. 33 (2000) 791;
A. Salomon, D. Cahen, S. Lindsay, J. Tomfohr, V.B. Engelkes, C.D. Frisbie, Adv. Mater. 15 (2003) 1881.

[6] J.M. Tour, Chem. Rev. 96 (1996) 537;
U.H.F. Bunz, Chem. Rev. 100 (2000) 1605;
T.M. Swager, in: F. Diederich, R.R. Tykwinski, P.J. Stang (Eds.), Acetylene Chemistry: Chemistry, Biology and Materials Science, Wiley–VCH, Weinheim, 2004.

[7] C. Devadoss, P. Bharathi, J.S. Moore, J. Am. Chem. Soc. 118 (1996) 9635;
J.S. Melinger, Y.C. Pan, V.D. Kleiman, Z.H. Peng, B.L. Davis, D. McMorrow, M. Lu, J. Am. Chem. Soc. 124 (2002) 12002.

[8] L.P. Yu, W.K. Chan, Z.H. Peng, A. Gharavi, Acc. Chem. Res. 29 (1996) 13;
Z.H. Peng, Angew. Chem., Int. Ed. 43 (2004) 930;
I.R. Whittall, A.M. McDonagh, M.G. Humphrey, M. Samoc, Adv. Organomet. Chem. 43 (1999) 349;
C. Weder, Chem. Commun. (2005) 5378.

[9] R.P. Hsung, C.E.D. Chidsey, L.R. Sita, Organometallics 14 (1995) 4808.

[10] R.D. Adams, T. Barnard, A. Rawlett, J.M. Tour, Eur. J. Inorg. Chem. 1 (1998) 429.

[11] W.M. Khairul, L. Porres, D. Albesa-Jove, M.S. Senn, M. Jones, D.P. Lydon, J.A.K. Howard, A. Beeby, T.B. Marder, P.J. Low, J. Cluster Sci. 17 (2006) 65.

[12] T. Ren, Organometallics 24 (2005) 4854.

[13] T. Ren, G.-L. Xu, Comments Inorg. Chem. 23 (2002) 355;
S.K. Hurst, T. Ren, J. Organomet. Chem. 670 (2003) 188.

[14] T. Ren, Organometallics 21 (2002) 732.

[15] G.-L. Xu, C. Campana, T. Ren, Inorg. Chem. 41 (2002) 3521.

[16] T. Ren, G. Zou, J.C. Alvarez, Chem. Commun. (2000) 1197;
G.-L. Xu, G. Zou, Y.-H. Ni, M.C. DeRosa, R.J. Crutchley, T. Ren, J. Am. Chem. Soc. 125 (2003) 10057;
Y. Shi, G.T. Yee, G. Wang, T. Ren, J. Am. Chem. Soc. 126 (2004) 10552.

[17] G.-L. Xu, M.C. DeRosa, R.J. Crutchley, T. Ren, J. Am. Chem. Soc. 126 (2004) 3728.

[18] G.-L. Xu, R.J. Crutchley, M.C. DeRosa, Q.-J. Pan, H.-X. Zhang, X. Wang, T. Ren, J. Am. Chem. Soc. 127 (2005) 13354.

[19] T.L. Schull, J.G. Kushmerick, C.H. Patterson, C. George, M.H. Moore, S.K. Pollack, R. Shashidhar, J. Am. Chem. Soc. 125 (2003) 3202;
S.A. Getty, C. Engtrakul, L. Wang, R. Liu, S.-H. Ke, H.U. Baranger, W. Yang, M.S. Fuhrer, L.R. Sita, Phys. Rev. B 71 (2005) 241401(R).

[20] A.S. Blum, T. Ren, D.A. Parish, S.A. Trammell, M.H. Moore, J.G. Kushmerick, G.-L. Xu, J.R. Deschamps, S.K. Pollack, R. Shashidhar, J. Am. Chem. Soc. 127 (2005) 10010.

[21] D.-H. Chae, J.F. Berry, S. Jung, F.A. Cotton, C.A. Murillo, Z. Yao, NanoLetters 6 (2006) 165;
S.Y. Lin, I.W.P. Chen, C.H. Chen, M.H. Hsieh, C.Y. Yeh, T.W. Lin, Y.H. Chen, S.M. Peng, J. Phy. Chem. B 108 (2004) 959.

[22] J.-W. Ying, D.R. Sobransingh, G.-L. Xu, A.E. Kaifer, T. Ren, Chem. Commun. (2005) 357.

[23] C.J. Yu, Y.C. Chong, J.F. Kayyem, M. Gozin, J. Org. Chem. 64 (1999) 2070.

[24] S.K. Pollack, J. Naciri, J. Mastrangelo, C.H. Patterson, J. Torres, M. Moore, R. Shashidhar, J.G. Kushmerick, Langmuir 20 (2004) 1838.

[25] S.K. Hurst, G.-L. Xu, T. Ren, Organometallics 22 (2003) 4118.

[26] G.-L. Xu, C.G. Jablonski, T. Ren, J. Organomet. Chem. 683 (2003) 388.

[27] F.A. Cotton, C.A. Murillo, R.A. Walton (Eds.), Multiple Bonds between Metal Atoms, third ed., Springer Science and Business Media Inc., New York, 2005.

[28] J.L. Bear, B. Han, S. Huang, K.M. Kadish, Inorg. Chem. 35 (1996) 3012;
J.L. Bear, Y. Li, B. Han, E.V. Caemelbecke, K.M. Kadish, Inorg. Chem. 36 (1997) 5449;
K.M. Kadish, T.D. Phan, L.-L. Wang, L. Giribabu, A. Thuriere, J. Wellhoff, S. Huang, E.V. Caemelbecke, J.L. Bear, Inorg. Chem. 43 (2004) 4825.

[29] C. Lin, T. Ren, E.J. Valente, J.D. Zubkowski, J. Chem. Soc., Dalton Trans. (1998) 571.

[30] S.K. Hurst, M.P. Cifuentes, J.P.L. Morrall, N.T. Lucas, I.R. Whittall, M.G. Humphrey, I. Asselberghs, A. Persoons, M. Samoc, B. Luther-Davies, A.C. Willis, Organometallics 20 (2001) 4664;
H.-Y. Chao, W. Lu, Y. Li, M.C.W. Chan, C.-M. Che, K.-K. Cheung, N. Zhu, J. Am. Chem. Soc. 124 (2002) 14696;
V.W.-W. Yam, C.-H. Tao, L. Zhang, K.M.-C. Wong, K.-K. Cheung, Organometallics 20 (2001) 453;
I.R. Whittall, M.G. Humphrey, D.C.R. Hockless, Aust. J. Chem. 50 (1997) 991;
I.R. Whittall, M.G. Humphrey, D.C.R. Hockless, Aust. J. Chem. 51 (1998) 219;
I.R. Whittall, M.P. Cifuentes, M.G. Humphrey, B. Luther-Davies, M. Samoc, S. Houbrechts, A. Persoons, G.A. Heath, D.C.R. Hockless, J. Organomet. Chem. 549 (1997) 127;
Y.Y. Lin, S.W. Lai, C.M. Che, K.K. Cheung, Z.Y. Zhou, Organometallics 21 (2002) 2275.

[31] M.I. Bruce, J. Davy, B.C. Hall, Y.J. van Galen, B.W. Skelton, A.H. White, Appl. Organomet. Chem. 16 (2002) 559.

[32] T. Ren, Coordin. Chem. Rev. 175 (1998) 43.

[33] G.-L. Xu, C.G. Jablonski, T. Ren, Inorg. Chim. Acta 343 (2003) 387.

[34] SAINT V 6.035, Software for the CCD Detector System, Bruker-AXS Inc., 1999.

[35] SHELXTL 5.03 (WINDOW-NT Version), Program Library for Structure Solution and Molecular Graphics, Bruker-AXS Inc., 1998.